Dyes and Pigments 92 (2012) 1184–1191

Contents lists available at SciVerse ScienceDirect

Dyes and Pigments

journal homepage: www.elsevier.com/locate/dyepig

Synthesis and study of nucleic acids interactions of novel monomethine cyanine dyes

Stefka Kaloyanova[a], Ivo Crnolatac[b,*], Nedyalko Lesev[a], Ivo Piantanida[b], Todor Deligeorgiev[a]

[a] Department of Applied Organic Chemistry, Faculty of Chemistry, University of Sofia, 1164 Sofia, Bulgaria
[b] Laboratory for Study of Interactions of Biomacromolecules, Division of Organic Chemistry and Biochemistry, Ruder Boskovic Institute, Bijenicka c. 54, 10000 Zagreb, Croatia

ARTICLE INFO

Article history:
Received 16 June 2011
Received in revised form
24 August 2011
Accepted 27 August 2011
Available online 3 September 2011

Keywords:
Cyanine dyes
DNA binding
Fluorescence
Thermal melting
Circular dichroism
Antiproliferation

ABSTRACT

Six asymmetric monomethine cyanine dyes have been synthesized and their spectral characteristics and interaction with double stranded (ds)DNA have been investigated for their prospective use as fluorescent markers in molecular biology. Therefore, the non-covalent binding of the compounds with dsDNA was explored. Apart from the fluorescence spectroscopy, the study includes UV/Vis spectrophotometry and circular dichroism spectroscopy, as well as the thermal melting experiments. Although the compounds show relatively low binding affinity toward dsDNA and do not have intrinsic fluorescence, in the presence of dsDNA they exhibited considerable enhancement in fluorescence intensity. Therefore the studied dyes show interesting platform for future modifications directed toward more sequence selective derivatives. The compound with the highest affinity toward dsDNA showed interesting anti-proliferative potential and specificity.

1. Introduction

Although the history of cyanine dyes covers more than century and a half [1], the interest in their synthesis and various applications are still present. Their use in molecular biology [2], medical [3], as well as, clinical analysis [4] has brought them once again into the limelight. The sensitivity of cyanine based fluorescent markers for DNA detection and characterization is almost equal to that of radioactive probes [5], which are less popular because of the safety concerns. The free cyanines in solution exhibit almost no intrinsic fluorescence, losing the absorbed energy through the torsional motion [6] or other nonradiative relaxation, however, upon DNA binding which results in rigidification of the dye structure, fluorescent intensity enhances significantly. The cyanine dyes are showing two predominant DNA binding modes: (1) intercalation between adjacent base pairs or bis-intercalation of some covalently bridged dimers, and (2) minor groove binding. This dual binding nature is in accordance with the theoretical observations considering that their structure implies (poly)methine bridge, which is flexible and allows twisting, following the curvature of the minor groove [7], with the planar heterocycles, prone to intercalation, on both sides. Therefore, the mode of the DNA binding can vary not only with the change of the heterocyclic nitrogen subunits or multiplicity of the methine bridge but also with the nature, charge and steric characteristic of the substituents.

2. Materials and methods

2.1. Materials

All starting compounds and solvents were commercial products from Sigma–Aldrich and were used without further purification, except for compounds **7a** [8] and **7d** [9], which were synthesized by modified known procedures.

2.2. Analysis methods and equipment

All products were characterized and/or compared with reported data. The progress of the reactions was monitored by TLC (Merck F 254 silica gel; dichloromethane: methanol: acetic acid, 86:13:1). ^{1}H-NMR spectra of the compounds that have not been reported previously were recorded on a Bruker Avance 600 MHz instrument in DMSO-d_6 as solvent. Elemental analyses were performed on a Vario III instrument. Melting points were determined on a Köfler apparatus and are uncorrected.

* Corresponding author. Tel.: +385 14561111/1537; fax: +385 14680195.
E-mail address: icrnolat@irb.hr (I. Crnolatac).

0143-7208/$ – see front matter © 2011 Elsevier Ltd. All rights reserved.
doi:10.1016/j.dyepig.2011.08.019

Table 1
^{1}H-NMR, elemental analysis, yields and melting points of dyes **a**–**d**.

Dye	Molecular formulas	Mw	Yield [%]	Melting point [°C]	Elemental analysis				^{1}H–NMR, 600 MHz, DMSO-d_6, δ (ppm)
					$N_{calc./found}$	$C_{calc./found}$	$S_{calc./found}$	$H_{calc./found}$	
a	$C_{25}H_{20}BrClN_2S.CH_3OH$	527.90	71	228–230 decomp.	5.31/5.12	59.15/58.95	6.32/5.94	4.58/4.13	4.25 (*s*, 3H, N^+CH_3), 5.77 (*s*, 2H, CH_2), 7.10 (*s*, 1H, CH), 7.28 (*t*, 3H, ArH), 7.36 (*t*, 2H, ArH), 7.57 (*d*, 1H, ArH), 7.78 (*d*, 1H, ArH), 7.86 (*d*, 1H, ArH), 8.51 (*d*, 1H, ArH), 8.55 (*d*, 1H, ArH), 8.64 (*d*, 1H, ArH), 8.68 (*d*, 1H, ArH), 8.75 (*d*, 1H, ArH)
b	$C_{30}H_{26}BrN_3O_2S.2CH_3OH$	636.60	60	245–247 decomp.	6.60/6.32	60.37/60.06	5.38/5.11	5.04/4.83	2.16 (*m*, 2H, CH_2), 2.35 (*s*, 3H, CH_3), 3.73 (*t*, 2H, CH_2), 4.25 (*s*, 3H, N^+CH_3), 4.51 (*t*, 2H, CH_2), 6.94 (*s*, 1H, CH), 7.58 (*t*, 1H, ArH), 7.84 (*m*, 3H, ArH), 7.87 (*m*, 2H, ArH), 8.01 (*d*, 1H, ArH), 8.26 (*d*, 1H, ArH), 8.35 (*s*, 1H, ArH), 8.43 (*s*, 1H, ArH), 8.47 (*d*, 1H, ArH), 8.50 (*d*, 1H, ArH)
c	$C_{27}H_{25}BrN_4O_2S.H_2O$	567.50	45	218–221 decomp.	9.87/10.12	57.14/57.66	5.65/5.47	4.80/4.13	2.36 (*s*, 3H, CH_3), 4.24 (*s*, 3H, N^+CH_3), 4.49 (*t*, 2H, CH_2), 4.74 (*t*, 2H, CH_2), 6.93 (*t*, 1H, ArH), 6.98 (*s*, 1H, CH), 7.22 (*t*, 2H, ArH), 7.35 (*d*, 2H, ArH), 7.58 (*t*, 1H, ArH), 7.84 (*t*, 1H, ArH), 8.01 (*d*, 1H, ArH), 8.10 (*d*, 1H, ArH), 8.35 (*s*, 1H, ArH), 8.45 (*s*, 1H, ArH), 8.47 (*d*, 1H, ArH), 8.51 (*d*, 1H, ArH), 9.68 (*s*, 1H, NH)
d	$C_{24}H_{26}ClIN_3S_2$	456.07	63	233–236 decomp.	7.21/6.89	49.45/49.16	11.00/10.84	4.50/4.19	2.10 (*s*, 4H, CH_2SCH_2), 2.38–2.42 (*m*, 4H, CH_2CH_2), 2.68 (*s*, 2H, S^+CH_2), 3.20–3.26 (*m*, 2H, CH_2), 3.50 (*s*, 3H, CH_3), 3.73 (*s*, 3H, N^+CH_3), 4.35–4.38 (*m*, 2H, NCH_2), 6.34 (*s*, 1H, CH), 7.54 (*d*, 2H, ArH), 7.69 (*d*, 1H, ArH), 8.02–8.05 (*m*, 2H, ArH), 8.38 (*d*, 1H, ArH), 8.48 (*d*, 1H, ArH), 8.53 (*d*, 1H, ArH)

2.3. Synthesis of cyanine dyes ***a***–***f***

2.3.1. General procedure for synthesis of dyes ***a***–***d***

In a reaction vessel equipped with magnetic stirrer equimolar amounts of intermediates **5a**–**5b** (0.001 mol) and **8a**–**8d** (0.001 mol) were suspended or dissolved in 10 ml ethanol. N-diisopropylethylamine (0.002 mol) was added and the reaction mixture was stirred at room temperature for 1–4 h. The progress of the reaction was monitored by TLC. The resulting precipitate was filtered off, washed with diethyl ether and air-dried. Dyes **a**–**d** were recrystallized from methanol.

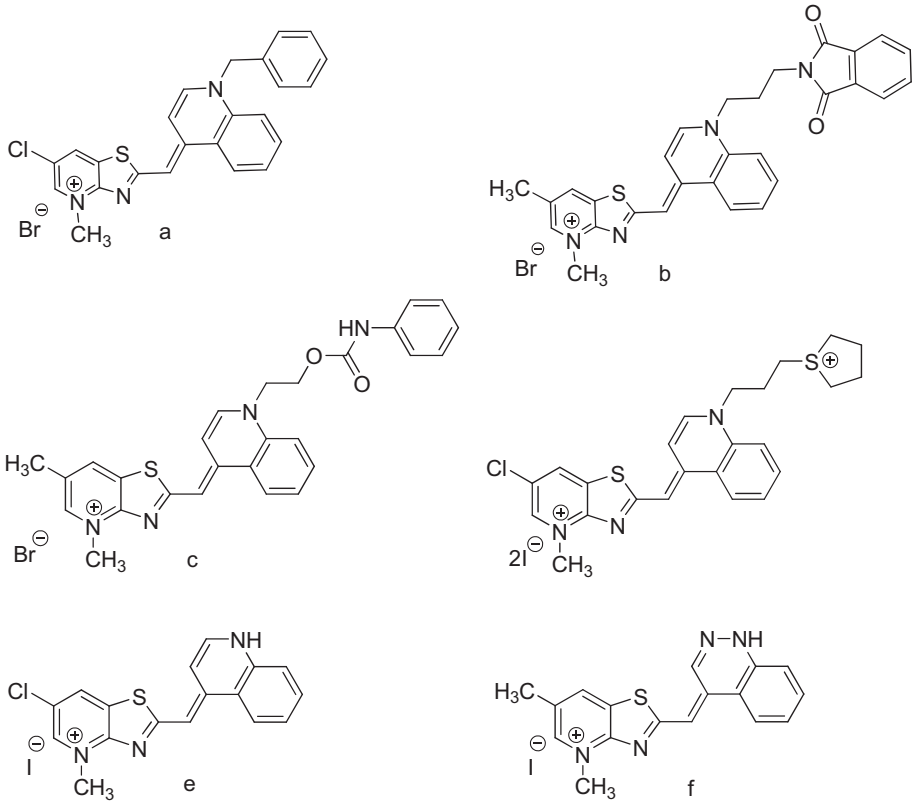

Scheme 1. Structures of studied compounds.

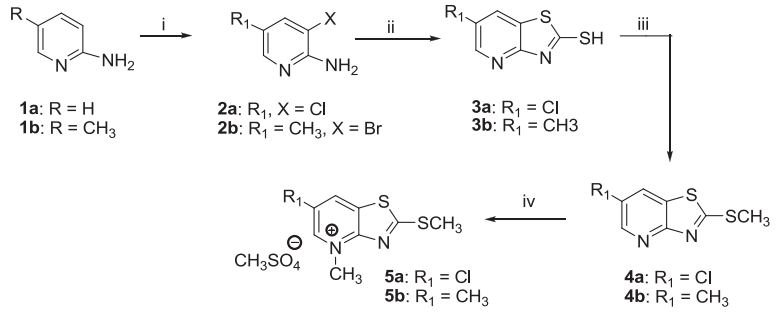

i: HCl or HBr, H_2O_2,70°C, 2-4 *hours*, 66-70% yield; ***ii***: potassium O-ethyl dithiocarbonate, glycerol, MW irradiation, 80-120W, 15-20 min, 89-92 % yield; ***iii***: N-Diisopropylethylamine, ultrasound irradiation, 67-71% yield; ***iv***: trichloroethylene, dimethyl sulfate (DMS), 30 *min*, reflux, 60-94% yield

Scheme 2. Synthesis of intermediates **5a** and **5b**.

2.3.2. Synthesis of dyes *e* and *f*

Dyes **e** and **f** were obtained by previously described synthetic procedure [10].

2.4. Study of DNA/RNA interactions

2.4.1. UV/Visible spectrophotometry, circular dichroism (CD) and fluorescence spectroscopy

The UV/Vis spectra were recorded on a Varian Cary 100 Bio spectrophotometer, fluorescence spectra on a Varian Cary Eclipse fluorescence spectrophotometer and CD spectra were collected with a Jasco J-810 spectropolarimeter at 25 °C using 1 cm path quartz cuvettes.

Absorption spectra to determine the extinction coefficients of the dyes were obtained on CECIL Aurius 3021 spectrophotometer in methanol (1×10^{-5} mol/l).

The polynucleotides: poly dAdT–poly dAdT, poly dA–poly dT, poly dG–poly dC, poly dGdC–poly dGdC, poly A–poly U, and *calf thymus* (*ct*)-DNA (Sigma–Aldrich, St.Louis, USA) were dissolved in sodium cacodylate buffer, $I = 0.05$ mol dm^{-3}, pH = 7, calf thymus (*ct*-) DNA was additionally sonicated and filtered through a 0.45 μm filter. Aqueous solutions of compounds were buffered to pH = 7 (sodium cacodylate buffer, $I = 0.05$ mol × dm^{-3}). The polynucleotide concentration was determined spectroscopically [11] as the concentration of phosphates. Spectrophotometric titrations were performed at pH = 7.0 (sodium cacodylate buffer, $I = 0.05$ mol dm^{-3}) by adding portions of polynucleotide solution into the solution of the studied compound. The CD experiments were performed by adding aliquots of the aqueous solutions of compounds into the solution of polynucleotide. In fluorimetric experiments the excitation wavelength above 500 nm ($\lambda_{exc} > 500$ nm) was used to avoid the possible inner filter effect caused by increasing absorbance of the polynucleotide. The emission spectra were collected in the range $\lambda_{em} = 510–650$ nm. The titration data were processed using Scatchard equation [12,13] the resulting values were in the range of $n = 0.3–0.1$ however, for the purpose of comparison all K_s values were re-calculated with the fixed value of $n = 0.2$. Values for K_s, given in Table 1, have acceptable correlation coefficients (>0.99).

2.4.2. Thermal denaturation experiments

Thermal melting curves for poly dAdT–poly dAdT, poly A–poly U and their complexes with studied compounds were determined as previously described [14] by following the change in the absorption at 260 nm as a function of temperature. The absorbance of the ligands was subtracted from each curve and the absorbance scale was normalized. *Tm* values are the midpoints of the transition curves, determined from the maximum of the first derivative and checked graphically by the tangent method. The Δ*Tm* values were calculated subtracting *Tm* of the free nucleic acid from *Tm* of the complex. The Δ*Tm* values (with the instrumental error ± 0.5 °C) reported are the average of at least duplicate measurements.

2.5. Bioassay

2.5.1. Cell culturing

The experiments were carried out on 2 human cell lines: H460 (lung carcinoma) and HCT 116 (colon carcinoma). Cells were cultured as monolayers and maintained in Dulbecco's modified Eagle medium (DMEM), supplemented with 10% fetal bovine serum (FBS), 2 mM L-glutamine, 100 U/ml penicillin and 100 μg/ml streptomycin in a humidified atmosphere with 5% CO_2 at 37 °C.

2.5.2. Proliferation assay

The panel cell lines were inoculated on day 0 onto a series of standard 96-well microtiter plates, at $1 \times 10^4–3 \times 10^4$ cells/ml, depending on the doubling times of specific cell line. Test agents

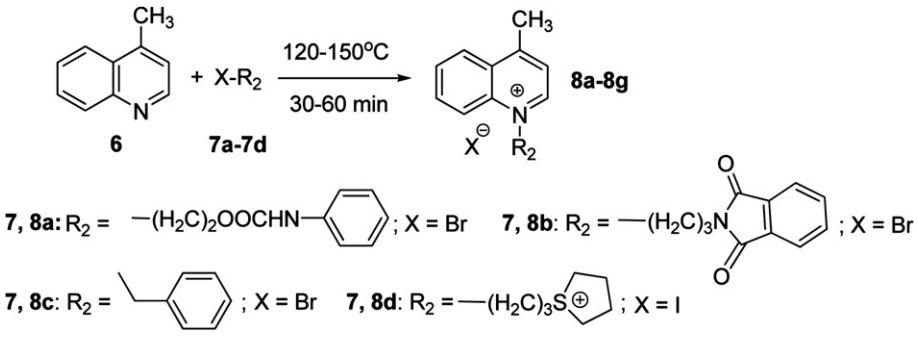

Scheme 3. Synthesis of intermediates **8a**–**8d**.

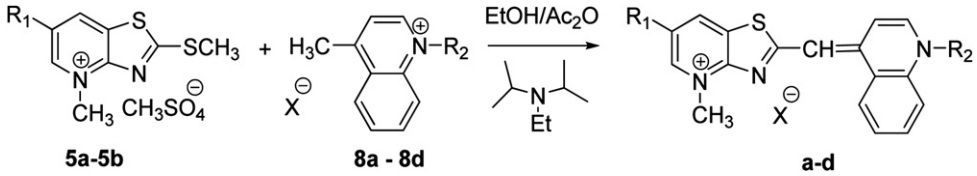

Scheme 4. Synthesis of dyes **a**–**d**.

were then added in five 10-fold dilutions (from 10^{-8} to 10^{-4} M) and incubated for a further 72 h. Working dilutions were freshly prepared on the day of testing. The solvent was also tested for possible inhibitory activity by adjusting its concentration to be the same as in working concentrations. After 72 h of incubation the cell growth rate was evaluated by the MTT assay [15], which detects dehydrogenase activity in viable cells. The MTT Cell Proliferation Assay is a colorimetric assay system, which measures the reduction of a tetrazolium component (MTT) into an insoluble formazan product by the mitochondria of viable cells. For this purpose the medium containing compound was discarded and medium with MTT was added to each well at a concentration of 20 μg MTT/40 μl. After 4 h of incubation the precipitates were dissolved in 160 μl of dymethyl-sulphoxide (DMSO). The absorbance (OD, optical density) was measured on a microplate reader at 570 nm. The absorbance is directly proportional to the cell viability. The percentage of growth (PG) of the cell lines was calculated according to one or the other of the following two expressions:

If $(\text{mean OD}_{\text{test}} - \text{mean OD}_{\text{tzero}}) \geq 0$ then

$$PG = 100 \times (\text{mean OD}_{\text{test}} - \text{mean OD}_{\text{tzero}})/(\text{mean OD}_{\text{ctrl}} - \text{mean OD}_{\text{tzero}})$$

If $(\text{mean OD}_{\text{test}} - \text{mean OD}_{\text{tzero}}) < 0$ then:

$$PG = 100 \times (\text{mean OD}_{\text{test}} - \text{mean OD}_{\text{tzero}})/\text{OD}_{\text{tzero}}$$

Where:

Mean OD_{tzero} = the average of optical density measurements before exposure of cells to the test compound.

Mean OD_{test} = the average of optical density measurements after the desired period of time.

Mean OD_{ctrl} = the average of optical density measurements after the desired period of time with no exposure of cells to the test compound.

Each test point was performed in quadruplicate in two individual experiments. The results were expressed as GI_{50}, a concentration necessary for 50% of inhibition. Each result is a mean value from at least two separate experiments.

3. Results and discussion

3.1. Synthesis and structural analysis of dyes *a*–*f*

Monomethine cyanine dyes are generally synthesized by the reaction of two heterocyclic quaternary salts, one bearing a reactive methyl group and the other a quaternized heterocycle containing a thioalkyl which is a good leaving group, in the presence of base [16]. As a part of our previously investigations into monomethine cyanine dyes, we developed novel method for their synthesis, using a mixture of a quaternary heterocyclic methylthio salt and non-quaternized heterocyclic compound bearing a reactive methyl group in solvent-free conditions and without the presence of a basic agent [10]. Both methods were used for obtaining of the dyes **a**–**f**.

Intermediates **5a** and **5b** were prepared according to the reported procedures [17–20] (Scheme 2).

2-Bromoethylphenyl carbamate (**7a)** was synthesized according to modified procedure [8] by refluxing phenylisocyanate and 2-bromoethanol in hexane for 3 h. Sulfonium salt (**7d)** was prepared from tetrahydrothiophene and 1,3-diiodopropan in acetone at room temperature [9]. Intermediates **8a**–**8d** were synthesized by quaternization of 4-methylquinoline (**6**) and the corresponding alkyl or aralkyl halides (**7a**–**7d**) under solvent-free conditions with the corresponding alkyl or aralkyl bromides and iodides (Scheme 3).

All intermediates are hygroscopic and their structures were proved along with the structures of the dyes by ^{1}H-NMR spectroscopy and elemental analyses.

Four novel monomethine cyanine dyes were synthesized in good to high yields and high purity by condensation of quaternized 4-methylqunolinium salts (**8a**–**8d**) with quaternized 2-methylthioheterocyclic salts (**5a**–**5b**) in the presence of a basic agent (N-diisopropylethylamine) and appropriate solvent, ethanol or acetic anhydride, at room temperature (Scheme 4). The dyes obtained were isolated as crude products by direct filtration in the cases where ethanol was the reaction solvent. When acetic anhydride was used as reaction solvent the dyes were isolated by precipitation with diethyl ether followed by filtration.

Dyes **e** and **f** were synthesized according to previously reported novel method [10] (Scheme 5).

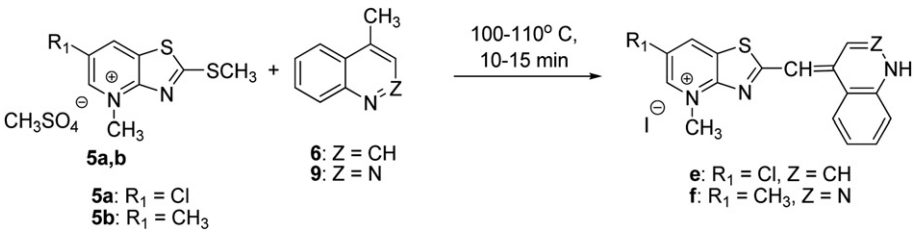

Scheme 5. Synthesis of dyes **e** and **f**.

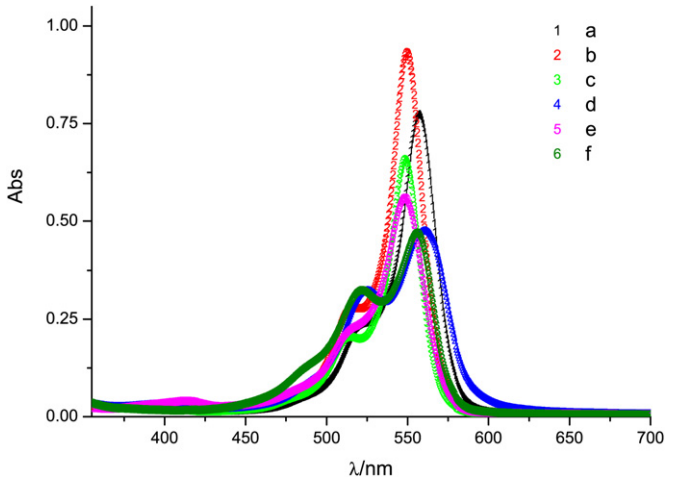

Fig. 1. UV/Vis spectra of compounds **a**, **b**, **c**, **d**, **e** and **f** in methanol (1×10^{-5} mol/l).

Table 2
Absorption maxima and extinction coefficients of dyes **a**–**f**.

Dye	λ_{max} [nm]	ε [l cm^{-1} mol^{-1}]
a	557	154,600
b	550	186,600
c	549	131,600
d	560	95,000
e	549	111,800
f	556	94,000

Dyes **a**–**f** were recrystallized from methanol to obtain the analytical samples. The structures of the four novel analogs of Thiazole Orange (**a**–**d**) were evaluated by ^{1}H-NMR spectroscopy and elemental analysis (Table 1). Reaction yields and melting points of the products are summarized in Table 1.

3.2. Physico-chemical properties of aqueous solutions of studied compounds

The absorption maxima and molar absorptivities of dyes **a**–**f** were determined in methanol solutions and are presented in the Fig. 1 and Table 2.

Studied compounds (Scheme 1) are moderately soluble in redistilled water (about $c = 1 \times 10^{-4}$ mol dm^{-3}). According to the spectrophotometry measurements, the aqueous solutions of **a, b, c, d, e,** and **f** were stable showed no significant change in their UV/Vis spectra over the period of two months. Furthermore, upon heating up to 90 °C, the UV/Vis spectra of all the studied compounds did not significantly change, the minor changes (less than 5%) were reversible after cooling back to room temperature. The UV/Vis absorption of aqueous solutions of **a**, **b, c, d, e** and **f** at their respective absorption maxima showed linear correlation to the concentrations up to $c = 2–4 \times 10^{-5}$ mol dm^{-3}, therefore indicating that there is no significant intermolecular stacking which otherwise would result in hypochromic shift. Aqueous solutions of **a, b, c, d, e** and **f** at $c = 1 \times 10^{-6}$ mol dm^{-3} (sodium cacodylate buffer, $I = 0.05$ mol dm^{-3}, pH = 7.0) exhibited negligible fluorescence upon excitation at their respective absorbance maxima.

3.3. Study of interactions of *a*, *b*, *c*, *d*, *e* and *f* with DNA and RNA

3.3.1. UV/Vis spectrophotometric titrations

Addition of ct-DNA resulted in batochromic and hypochromic shifts in UV/Vis spectra of **a**, **b**, **d** (Figs. 2–4), no distinct isosbestic point could be observed, which suggests mixed binding mode.

Using UV/Vis spectrophotometric data obtained by titration of compounds with ct-DNA solution, the binding constants K_s and ratios $n_{[\text{bound compound}]/[\text{ct-DNA}]}$ were calculated by Scatchard equation [11,12]. However only with the data acquired by titration of **a** and **b**, the equation gave meaningful results, with the n ratio fixed at 0.5, compounds **a** and **b** showed similar binding constant (log $K_s = 5.41$ and 5.39, respectively).

3.3.2. Fluorescence spectroscopy

Although compounds **a**, **b**, **c**, **d**, **e** and **f** did not exhibit considerable intrinsic fluorescence, the fluorescence intensity, compound solutions increased upon addition of *ct*-DNA (Fig. 5). The increase of fluorescence intensity was relatively strong with all the compounds, except with **b**, where the increase was quite weak (up to 30 a.u.). Due to the quite complex pattern of events involved in fluorescence increase upon binding to DNA the strength of emission increase could not be directly correlated to the binding affinity. Strong fluorescence of complexes enabled fluorimetric titrations and calculation of the binding constants (log K_s) and ratio $n_{[\text{bound compound}]/[\text{ct-DNA}]}$ that are given in Table 3. Fluorimetric titrations were performed in buffered (pH = 7.0) aqueous solution, at the wavelength range (λ_{exc} = 550 nm, $\lambda_{emission}$ = 560–700 nm), significantly distanced from the absorbance range of the ct-DNA (λ = 220–300 nm).

The majority of the compounds in the study do not show high binding affinities (K_s values) toward ct-DNA, however the increase

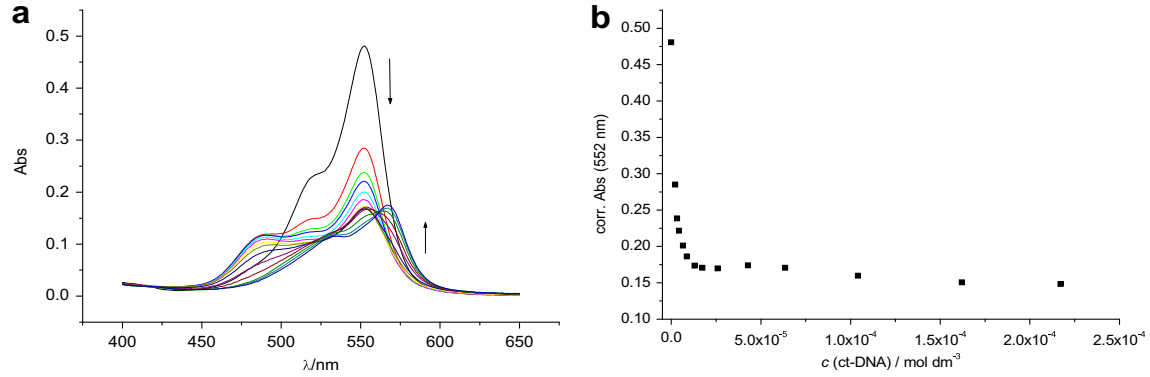

Fig. 2. a) UV/Vis titration of **a** ($c = 2.4 \times 10^{-5}$ mol dm^{-3}) with ct-DNA; b) Changes in UV/Vis spectra of **a** at λ_{max} = 552 nm upon titration with ct-DNA, at pH = 7, sodium cacodylate buffer, $I = 0.05$ mol dm^{-3}.

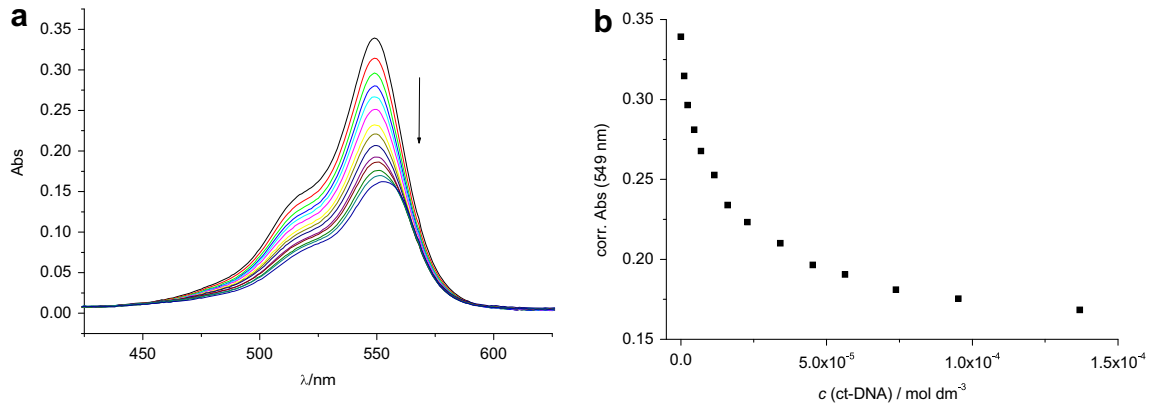

Fig. 3. a) UV/Vis titration of **b** ($c = 2.4 \times 10^{-5}$ mol dm^{-3}) with *ct*-DNA; b) Changes in UV/Vis spectra of **b** at $\lambda_{max} = 549$ nm upon titration with *ct*-DNA, at pH = 7, sodium cacodylate buffer, $I = 0.05$ mol dm^{-3}.

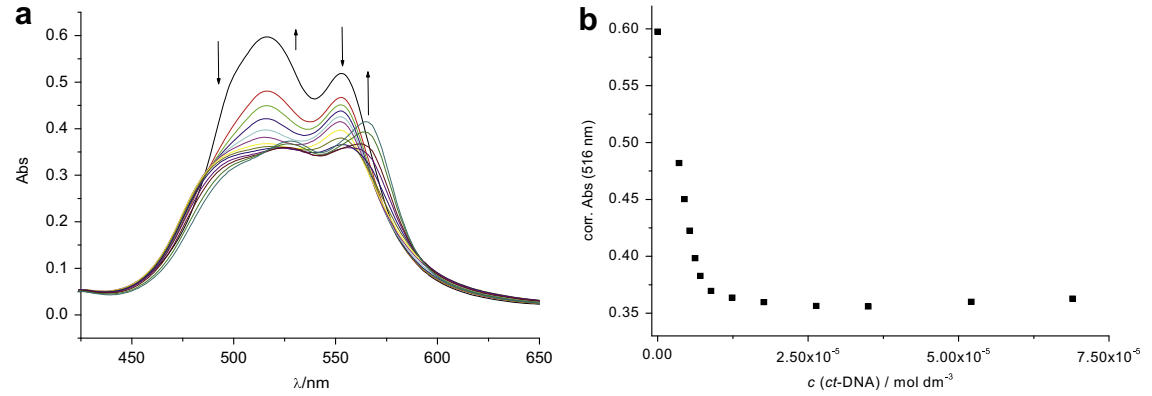

Fig. 4. a) UV/Vis titration of **d** ($c = 3.1 \times 10^{-5}$ mol dm^{-3}) with *ct*-DNA; b) Changes in UV/Vis spectra of **d** at $\lambda_{max} = 516$ nm upon titration with *ct*-DNA, at pH = 7, sodium cacodylate buffer, $I = 0.05$ mol dm^{-3}.

of the fluorescence intensity upon ct-DNA binding is considerable. The exceptions are: **b** which along with the low K_s value also exhibits quite low increase of the fluorescence intensity and **d** which actually shows relatively high K_s value and not so

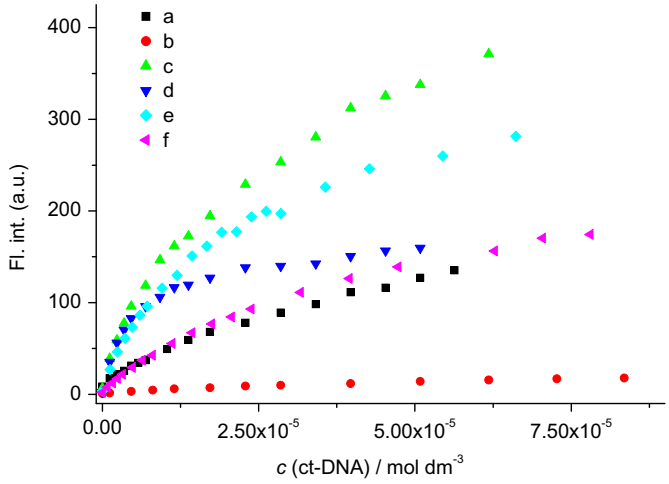

Fig. 5. Changes of fluorescence emission intensity of **a**, **b**, **c**, **d**, **e** and **f** (compound concentration, $c = 1 \times 10^{-6}$ mol dm^{-3}) at their respective maxima upon addition of ct-DNA at pH 7 (Na-cacodylate buffer, pH = 7.0, $I = 0.05$ M).

Table 3
Stability constants (log K_s),[a] ratios n = [bound compounds]/[polynucleotide][a] and spectroscopic properties of complexes[b] of **a**–**f** with ds-polynucleotides calculated according to fluorimetric titrations (Na-cacodylate buffer, $c = 0.05$ mol dm^{-3}, pH = 7.0, $\lambda_{exc} = 550$ nm, $\lambda_{em} = 560$–700 nm, slits 5 nm, c(fcompound) $= 1 \times 10^{-6}$ mol dm^{-3}).

		log K_s	n	ΔI_{calc}[b]	$\Delta\lambda$ nm[c]
a $\lambda_{exc} = 550$ nm	ct-DNA	5.28	fix 0.1	243	31
		4.93	fix 0.2	252	
b $\lambda_{exc} = 550$ nm	ct-DNA	5.29	fix 0.1	27.5	20
		4.94	fix 0.2	28.3	
c $\lambda_{exc=}550$ nm	ct-DNA	5.53	fix 0.1	505	18
		5.16	fix 0.2	525	
		5.06	fix 0.25	529	
		4.73	fix 0.5	537	
d $\lambda_{exc=}550$ nm	ct-DNA	6.51	fix 0.1	127	31
		6.03	fix 0.2	142	
		5.90	fix 0.25	145	
		5.54	fix 0.5	152	
e $\lambda_{exc=}550$ nm	ct-DNA	5.82	fix 0.1	327	21
		5.42	fix 0.2	344	
		5.31	fix 0.25	346	
		4.97	fix 0.5	352	
f $\lambda_{exc=}550$ nm	ct-DNA	5.40	fix 0.1	262	31
		5.05	fix 0.2	271	
		4.94	fix 0.25	273	
		4.62	fix 0.5	276	

[a] Titration data were processed using Scatchard equation, coefficients of correlation were >0.989–0.999 for all calculated K_s.
[b] Emission change; $\Delta I_{calc} = I_{lim} - I_0$; emission intensity change, calculated from titration data that were processed using Scatchard equation, where I_0 is calculated intensity of examined compound, while I_{lim} is calculated intensity of complex.
[c] $\Delta\lambda$, "Stokes shift", the difference between λ_{exc} and λ_{max} emission.

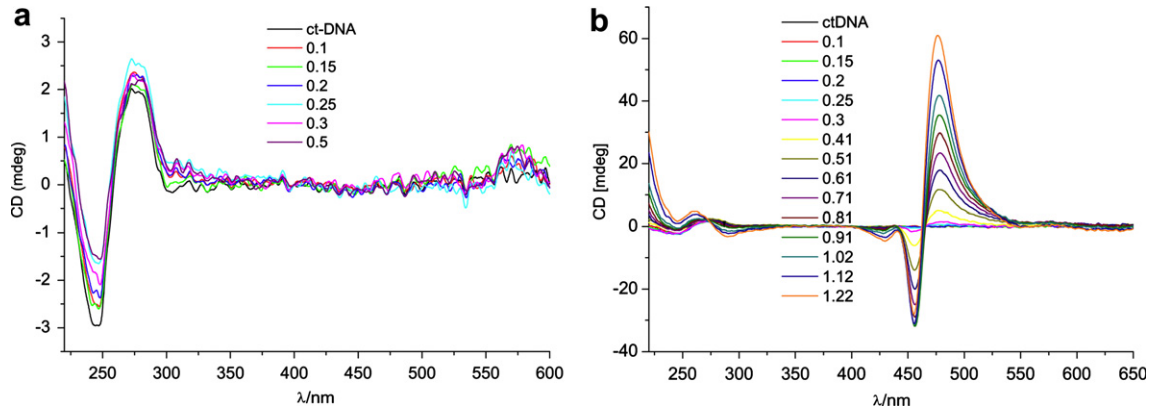

Fig. 6. CD titration of ct-DNA ($c = 2.0 \times 10^{-5}$ mol dm^{-3}) with **d** and **f** at molar ratios r = [compound]/[polynucleotide] (pH = 7.0, buffer sodium cacodylate, $I = 0.05$ mol dm^{-3}).

prominent fluorescence increase. However, due to quite complex pattern of physical events involved in fluorescence increase upon binding to DNA the strength of emission increase could not be directly correlated to binding affinity.

3.3.3. Thermal melting experiments

It is well known that upon heating ds-helices of polynucleotides at well-defined temperature (*Tm* value) dissociate into two single stranded polynucleotides. Non-covalent binding of small molecules to ds-polynucleotides usually has certain effect on the thermal stability of helices thus giving different *Tm* values. Difference between *Tm* value of free polynucleotide and complex with small molecule (ΔTm value) is important factor in characterization of small molecule/ds-polynucleotide interactions.

With the exception of **d**, the compounds did not stabilize the double helix of poly dAdT–poly dAdT or poly A–poly U. The compound **d** showed stabilization effect with p(dA–dT)$_2$ increasing with the increase of the concentration ratio r (r = [compound]/[polynucleotide] = 0.1, 0.2 and 0.3; ΔTm = 2.1, 5.9 and 11.3, respectively), while in the case of pApU no effect was observed with the concentration ratios ($r = 0.3$) used in the experiment.

3.3.4. Circular dichroism (CD) experiments

So far, non-covalent interactions at 25 °C were studied by monitoring the spectroscopic properties of studied compound upon addition of the polynucleotides. In order to get insight into the changes of polynucleotide properties induced by small molecule binding, we have chosen CD spectroscopy as a highly sensitive method toward conformational changes in the secondary structure of polynucleotides [21] In addition, achiral small molecules can eventually acquire induced CD spectrum (ICD) upon binding to polynucleotides, which could give useful information about modes of interaction [22]. It should be noted that studied compounds are achiral and therefore do not possess intrinsic CD spectrum.

Except for the compound **f** addition of all the compounds used in the study did not result in ICD effect (Fig. 6). The CD response upon addition of dye **d** to DNA was located at the wavelength range where both DNA and dye absorb (220–300 nm), which complicated the deconvolution of effects. However, especially significant decrease (from −3 to −1.5, which makes 50%) of CD intensity at 240–250 nm clearly pointed to significant distortion of DNA backbone and supported strong binding of **d** to DNA. The absence of induced CD (ICD) bands at longer wavelengths where only **d** absorbs (>450 nm) could result from several co-existing binding modes of **d** to DNA, which is actually in accordance with clear deviation from the isosbestic points noted in UV/Vis titrations (Fig. 4). For instance, binding of **d** into DNA minor groove should result in positive ICD band and intercalation of **d** should yield negative ICD band [23], whereby at experimental conditions used these two ICD effects could neutralize each other, thus yielding negligible spectral change.

Although compound **f** induces huge ICD effect with ct-DNA (as well as with some other synthetic polynucleotides, results not shown), this happens only at higher concentration ratios *r*. Such bisignate ICD signals at higher concentration ratios indicate non-specific binding along the DNA backbone [23].

3.4. Proliferation assay

Considering the overall low binding affinities and DNA/RNA stabilization effects of the compounds, only compound **d** was checked for its anti-proliferation effect on human cancer cell lines. The compound showed promising biological activity, exhibiting order of magnitude higher effect on colon carcinoma (HCT 116, $GI_{50} = 5 \pm 2$ μM) than toward lung cancer cell line (H460, $GI_{50} = 50 \pm 35$ μM), the specificity which could be of interest.

4. Conclusions

Six mono and di-cationic unsymmetrical cyanine dyes based on thiazolopyridinium (**a**–**d**) and quinolinium (**e**) or cinnolinium (**f**) moieties were synthesized. Four of the dyes are novel (**a**–**d**). All except one of them show significant fluorescence increase with the addition of ct-DNA, which renders their potential in nucleic acid analysis and detection, however further modification is needed since majority of the compounds (with the exception of **d**) show relatively low binding affinity toward ct-DNA, having 60:40 GC over AT ratio, and do not stabilize synthetic AT–AT sequence DNA or A–U sequence RNA against thermal denaturation, therefore demonstrating ineffective interaction with the polynucleotides. Along with the absence of the significant changes of the CD spectra of ct-DNA upon addition of the compounds, the UV/Vis, fluorescence spectrophotometric and thermal denaturation assays are all indicating weak interaction with the DNA/RNA helices. Although, the compound with the cinnolinium heterocycle, compound **f**, showed pronounced induced effect (ICD) on the CD spectra of ct-DNA and other polynucleotides (poly dAdT–poly dAdT, poly dA–poly dT, poly dG–poly dC, poly dGdC–poly dGdC and poly A–poly U), the character and the intensity of the ICD signal, as well as the fact that the basepair sequence has no effect on the occurrence of the ICD signal, points toward non-specific binding. Introduction of additional cationic charge (compound **d**) induced stronger binding, with higher affinity and also resulted in significant anti-proliferative effect on human cancer cell lines. In that way

emphasizing the importance of electrostatic interaction with the nucleic acids phosphate backbone and illustrating the direction for future modifications. Furthermore the anti-proliferative effect of compound **d** was rather selective, showing GI_{50} value an order of magnitude lower for colon carcinoma than for lung cancer cell line.

Acknowledgments

The authors thank Dr. Marijeta Kralj and Lidija Uzelac (Laboratory for experimental therapy, Division of Molecular Medicine, Ruder Boskovic Institute) for their work on experiments for determination of anti-proliferation effect of the compounds.

Appendix. Supplementary data

Supplementary data related to this article can be found online at doi:10.1016/j.dyepig.2011.08.019.

References

[1] Williams CHG. Researches on chinoline and its homologues. Trans R Soc Edinb Earth Sci 1856;21:377.
[2] Glazer AN, Rye HS. Stable dye–DNA intercalation complexes as reagents for high-sensitivity fluorescence detection. Nature 1992;359(6398):859–61.
[3] Carreon JR, Stewart KM, Mahon KP, Shin S, Kelley SO. Cyanine dye conjugates as probes for live cell imaging. Bioorg Med Chem Lett 2007;17(18):5182–5.
[4] Socher E, Jarikote DV, Knoll A, Roglin L, Burmeister J, Seitz O. FIT probes: peptide nucleic acid probes with a fluorescent base surrogate enable real-time DNA quantification and single nucleotide polymorphism discovery. Anal Biochem 2008;375(2):318–30.
[5] Rye HS, Yue S, Wemmer DE, Quesada MA, Haugland RP, Mathies RA, et al. Stable fluorescent complexes of double-stranded DNA with bis-intercalating asymmetric cyanine dyes – properties and applications. Nucleic Acids Res 1992;20(11):2803–12.
[6] Nygren J, Svanvik N, Kubista M. The interactions between the fluorescent dye thiazole orange and DNA. Biopolymers 1998;46(1):39–51.
[7] Armitage BA. Cyanine dye–DNA interactions: intercalation, groove binding, and aggregation. Top Curr Chem 2005;253:55–76.
[8] Baker JW, Davies MM, Gaunt J. The mechanism of the reaction of aryl isocyanates with alcohols and amines. Part IV. The evidence of infra-red absorption spectra regarding alcohol–amine association in the base-catalysed reaction of phenyl isocyanate with alcohols. J Chem Soc; 1949:24–7.
[9] Deligeorgiev T, Vasilev A, Drexhage K-H. Synthesis of novel monomeric cyanine dyes containing 2-hydroxypropyl and 3-chloro-2-hydroxypropyl substituents – Noncovalent labels for nucleic acids. Dyes Pigm 2007;73:69–75.
[10] Deligeorgiev T, Kaloyanova S, Vasilev A. A novel general method for preparation of neutral monomethine cyanine dyes. Dyes Pigm 2011;90:170–6.
[11] Malojcic G, Piantanida I, Marinic M, Zinic M, Marjanovic M, Kralj M, et al. A novel bis-phenanthridine triamine with pH controlled binding to nucleotides and nucleic acids. Org Biomol Chem 2005;3(24):4373–81.
[12] Scatchard G. The attractions of proteins for small molecules and ions. Ann NY Acad Sci 1949;51:660–72.
[13] Mc Ghee JD, von Hippel PH. Theoretical aspects of DNA-protein interactions: co-operative and non-co-operative binding of large ligands to a one-dimensional homogeneous lattice. J Mol Biol 1974;86:469–89.
[14] Chaires JB, Dattagupta N, Crothers DM. Studies on interaction of anthracycline antibiotics and deoxyribonucleic-acid – equilibrium binding-studies on interaction of daunomycin with deoxyribonucleic-acid. Biochemistry 1982; 21(17):3933–40.
[15] Mickisch G, Fajta S, Bier H, Tschada R, Alken P. Cross-resistance patterns related to glutathione metabolism in primary human renal-cell carcinoma. Urol Res 1991;19(2):99–103.
[16] Brooker LGS, Keyes G, Williams W. Color and constitution. V.1 the absorption of unsymmetrical cyanines. Resonance as a basis for a classification of dyes. J Am Chem Soc 1942;64:199–209.
[17] Dunn AD, Currie A, Hayes LE. Bromination of pyridines. II. Bromination of aminopicolines. J Prakt Chem 1989;331:369–544.
[18] Huang W, Tan Y, Ding M-W, Yang G- F. Improved synthesis of 2-(3*H*)benzothiazolethiones under microwave irradiation. Synth Commun 2007;37: 369–76.
[19] Deligeorgiev T, Kaloyanova S, Lesev N, Vaquero JJ. An easy and fast ultrasonic selective S-alkylation of hetaryl thiols at room temperature. Ultrason Sonochem 2010;17:783–8.
[20] Deligeorgiev T, Gadjev N, Vasilev A, Drexhage K-H, Yarmoluk SM. Synthesis of novel monomeric and homodimeric cyanine dyes with thioacetyl substituents for nucleic acid detection. Dyes Pigm 2007;72:28–32.
[21] Rodger A, Norden B. Circular dichroism and linear dichroism. New York: Oxford University Press; 1997 [Chapter 2].
[22] Garbett NC, Ragazzon PA, Chaires JB. Circular dichroism to determine binding mode and affinity of ligand-DNA interactions. Nat Protoc 2007;2(12): 3166–72.
[23] Eriksson M, Norden B. Linear and circular dichroism of drug-nucleic acid complexes. Meth Enzymol 2001;340:68–98.